Computational polyconvexification of isotropic functions

Timo Neumeier, Malte A. Peter, Daniel Peterseim, David Wiedemann

COMPUTATIONAL POLYCONVEXIFICATION OF ISOTROPIC FUNCTIONS[*]

TIMO NEUMEIER[†], MALTE A. PETER[‡], DANIEL PETERSEIM[‡], AND
DAVID WIEDEMANN[§]

Abstract. Based on the characterization of the polyconvex envelope of an isotropic function by its signed singular value representation, we propose a simple algorithm for the numerical approximation of the polyconvex envelope. Instead of operating on the lifted space of $d \times d$ matrices, the algorithm requires only the computation of the convex envelope of a function on a d-dimensional manifold, which is easily realized by standard algorithms. The significant speedup associated with the dimensional reduction from d^2 to d is demonstrated in a series of numerical experiments.

Key words. polyconvex envelope, convexification, numerical relaxation, isotropy

MSC codes. 49J45, 49J10, 74G65, 74B20

DOI. 10.1137/23M1589773

1. Introduction. Many applications in the field of nonlinear elasticity aim at finding a global minimizer of functionals of the form

$$(1.1) \qquad I(u) = \int_\Omega W\left(\nabla u(x)\right) \, \mathrm{d}x$$

over a domain $\Omega \subset \mathbb{R}^d$ in spatial dimension $d \in \{2, 3\}$ for a suitable weak class of deformations $u : \Omega \to \mathbb{R}^d$. In many relevant cases, the density $W : \mathbb{R}^{d \times d} \to \mathbb{R}_\infty := \mathbb{R} \cup \{\infty\}$ does not satisfy a suitable notion of convexity, and the existence of minimizers cannot be guaranteed. In fact, the infimum may not be reached, and nonconvexity, e.g., a multiwell structure of the energy density, may lead to the emergence of increasingly fine microstructures within the minimizing sequences. Moreover, the application of standard discretization methods for the minimization of I typically leads to mesh-dependent results with oscillations in the discrete deformation gradient at the length scale of the mesh size. Therefore, alternative approaches are introduced for both mathematical analysis and numerical simulation using relaxed formulations that focus on macroscopic features responsible for global behavior by extracting the relevant information from the unresolved microstructures [BCHH04, CD18, KNM+22, KNP+23, BKN+23].

[†]Institute of Mathematics, University of Augsburg, 86135 Augsburg, Germany (timo.neumeier@uni-a.de).

[‡]Institute of Mathematics and Centre for Advanced Analytics and Predictive Sciences AAPS, University of Augsburg, 86135 Augsburg, Germany (malte.peter@uni-a.de, daniel.peterseim@uni-a.de).

[§]Institute of Mathematics, University of Augsburg, 86135 Augsburg, Germany. Current Address: Fakultät für Mathematik, TU Dortmund, 44221 Dortmund, Germany (david.wiedemann@tu-dortmund.de).

The direct method in the calculus of variations links the limit behavior of a minimizing sequence of I to the minimizer of the function when W is replaced by its quasiconvex envelope W^{qc}; see [Dac82, AF84] and [Mül99, Dac08, Rou20] for an overview. Since the quasiconvex envelope W^{qc} is rarely known explicitly or even approximately, lower and upper bounds of W^{qc} and their numerical approximation are of great significance in computational nonlinear elasticity. While the rank-one convex envelope provides an upper bound, a lower bound of W^{qc} is provided by the polyconvex envelope W^{pc}. The notion of quasiconvexity requires growth conditions for the existence of a minimizer, which reflect a rather unphysical behavior in the compression regime $(\det(F) \to 0)$. Such growth conditions are not necessary under polyconvexity [Bal76, Bal77], and therefore polyconvexity is favorable for applications in nonlinear elasticity [Bal02]. Overall, the accurate approximation of polyconvex envelopes is of great importance for the practical realization of relaxation techniques.

In the context of elasticity, the main challenge for the efficient computation of semiconvex envelopes like polyconvex ones arises from the high-dimensional nature of the problem. Even the accurate numerical representation of the original density W requires a mesh of a domain in $d \times d$-dimensional space. For $d = 2$, this is already challenging but just about feasible with known linear programming algorithms for approximating the polyconvex envelope [Bar05, EBG13, BEG15]. However, even these efficient algorithms become practically infeasible for many relevant problems in $d = 3$ spatial dimensions.

In this work, we will therefore abandon the generality of these methods in favor of faster algorithms by restricting ourselves to the subclass of isotropic functions W. These functions model a directionally independent local material response. The relaxation of isotropic energy densities by polyconvexification is of fundamental engineering interest since classical energies, such as the Saint Venant–Kirchhoff density, are also non-polyconvex [Rao86]. More complex material models, for example, isotropic damage [BO12], suffer even more from nonconvexity.

Isotropic functions can be identified with a function $\Phi : \mathbb{R}^d \to \mathbb{R}_\infty$ by means of the vector of signed singular values $\nu(F) \in \mathbb{R}^d$ of F, namely, $W(F) = \Phi(\nu(F))$. In order to utilize this dimension reduction, it becomes desirable to characterize also polyconvexity in terms of Φ. Due to the high relevance of isotropic functions in nonlinear elasticity, this task was already addressed during the introduction of polyconvexity in [Bal77], and a sufficient condition for the polyconvexity in terms of the singular values was derived there. However, it is a priori not necessary and thus not suited for the computation of the polyconvex envelope. Sufficient and necessary conditions are presented for $d = 2$ in [Š97, Ros98, Š99] and for $d = \{2,3\}$ in [Mie05]. However, these conditions are not directly accessible for the numerical polyconvexification due to their implicit structure. For $d = 2$, a characterization of finite isotropic polyconvex functions by means of merely a convex symmetric function was presented in [DM06]. Finally, for $d \in \{2,3\}$, such a characterization was achieved in [WP23], which can handle also functions attaining infinity. This characterization corresponds to the definition of polyconvexity restricted to the set of diagonal matrices and thus can be considered optimal for isotropic functions. For functions arising in linear elasticity, related results on dimension reduction are derived in [BKS19].

The characterization of polyconvexity of isotropic functions presented in [WP23] leads to a simple algorithm for approximating their polyconvex envelope. Given a mesh of a d-dimensional domain of signed singular values, the algorithm simply lifts the mesh to a d-dimensional manifold embedded in three- and seven-dimensional space for $d = 2$ and $d = 3$, respectively. The subsequent computation of the convex envelope can be easily done with various algorithms, such as `Quickhull` [BDH96] or

the ones based on linear programming mentioned above. The computational effort is determined by the number of mesh points, which scales as in d-dimensional space. This dimensional reduction from $d \times d$ to d dimensions makes the novel algorithms feasible for the approximation of the polyconvex envelopes even for engineering applications in three dimensions.

The paper is organized as follows. In section 2, basic definitions, the analytical theory of polyconvexity, as well as the characterization of polyconvexity in terms of the signed singular values based on [WP23] are presented. Afterward, in section 3, the numerical realization of the polyconvexification approach, i.e., discretization and algorithmic treatment, is discussed. In section 4, a collection of numerical experiments shows the feasibility of the algorithms even in three spatial dimensions. Moreover, we numerically investigate polyconvexity properties of a parameter-dependent family of exponentiated Hencky-logarithmic energy densities [NLG$^+$15] beyond existing mathematical results. We conclude with some remarks in section 5.

2. Polyconvexification of isotropic functions. Let $d \in \{2,3\}$, and let $W : \mathbb{R}^{d \times d} \to \mathbb{R}_\infty := \mathbb{R} \cup \{\infty\}$ be a function which maps $d \times d$ matrices to real scalars or infinity. We think of energy densities in functionals of the form (1.1). The possible value infinity models practically unrealizable states of the deformation gradient. We are interested in the polyconvex envelope W^{pc} of the function W. The notion of polyconvexity relies on the minors of matrices $F \in \mathbb{R}^{d \times d}$. Given the determinant $\det(F)$ and the adjoint $\mathrm{adj}(F)$ of F, let

$$(2.1) \qquad \mathcal{M}(F) := \begin{cases} (F, \det(F)) & \text{if } d = 2, \\ (F, \mathrm{adj}(F), \det(F)) & \text{if } d = 3 \end{cases}$$

denote the minors of F. Since for $d = 2$ we identify $\mathbb{R}^{2 \times 2} \times \mathbb{R} \cong \mathbb{R}^5$ and for $d = 3$ we identify $\mathbb{R}^{3 \times 3} \times \mathbb{R}^{3 \times 3} \times \mathbb{R} \cong \mathbb{R}^{19}$, $\mathcal{M}(F)$ is considered as a vector of dimension $K_d = 5$ if $d = 2$ and $K_d = 19$ if $d = 3$. A function $V : \mathbb{R}^{d \times d} \to \mathbb{R}_\infty$ is said to be polyconvex if there exists a convex function $G : \mathbb{R}^{K_d} \to \mathbb{R}_\infty$ such that for all $F \in \mathbb{R}^{d \times d}$,

$$(2.2) \qquad V(F) = G(\mathcal{M}(F)).$$

The polyconvex envelope $W^{\mathrm{pc}} : \mathbb{R}^{d \times d} \to \mathbb{R}_\infty$ of W, defined by the pointwise supremum

$$(2.3) \qquad W^{\mathrm{pc}}(F) := \sup \left\{ V(F) \mid V : \mathbb{R}^{d \times d} \to \mathbb{R}_\infty \text{ polyconvex}, V \le W \right\},$$

is the largest polyconvex function below W. It is equivalently characterized by

$$W^{\mathrm{pc}}(F) = \sup \left\{ (G \circ \mathcal{M})(F) \mid G : \mathbb{R}^{K_d} \to \mathbb{R}_\infty \text{ convex}, G \circ \mathcal{M} \le W \right\}.$$

For a given function W, we define the (not necessarily convex) function $H : \mathbb{R}^{K_d} \to \mathbb{R}_\infty$ by

$$(2.4) \qquad H(X) := \begin{cases} W(F) & \text{if } X = \mathcal{M}(F), \\ \infty & \text{if } X \notin \mathcal{M}(\mathbb{R}^{d \times d}), \end{cases}$$

which is well-defined since $\mathcal{M}$ is injective. The polyconvex envelope W^{pc} of W is equal to the convex envelope H^{c} of H, i.e.,

$$(2.5) \qquad W^{\mathrm{pc}}(F) = H^{\mathrm{c}}(\mathcal{M}(F)).$$

Note that for finite-valued functions, convexity implies continuity. This is not the case for functions taking the value ∞. However, for the study of the functional

(1.1), it is important that the function G in the definition of polyconvexity (2.2) is lower semicontinuous (lsc). In this sense, we call a function V lower semicontinuous polyconvex (lsc-pc) if G in (2.2) is additionally lower semicontinuous. Note that this definition extends the classical definition of polyconvexity. In the physically relevant case that $W(F) = \infty$ for $\det(F) \leq 0$, $W(F) < \infty$ for $\det(F) > 0$, and $W(F) \to \infty$ for $\det(F) \to 0_+$, the function W is polyconvex if and only if W is lower semicontinuous polyconvex. This holds also for the case that $W(F)$ is finite if and only if $\det(F) \in [a, b] \subset \mathbb{R}$, which covers the case of isochoric functions, i.e., $a = b = 1$. Accordingly, we define the lower semicontinuous polyconvex envelope $W^{\mathrm{lsc\text{-}pc}}$ of W to be the largest lower semicontinuous polyconvex function below W.

In this paper, we restrict ourselves to the study of polyconvexity of isotropic functions. According to [Bal76], $W : \mathbb{R}^{d \times d} \to \mathbb{R}_\infty$ is called *objective* if $W(F) = W(RF)$ for all $F \in \mathbb{R}^{d \times d}$ and for all $R \in \mathcal{SO}(d)$, where $\mathcal{SO}(d)$ denotes the special orthogonal group of $d \times d$ matrices. Furthermore, W is called *isotropic* if W is objective and $W(F) = W(QFQ^T)$ holds for all F and for all $Q \in \mathcal{O}(d)$, the group of orthogonal $d \times d$ matrices. Therefore, W is isotropic if and only if

$$W(F) = W(R_1 F R_2)$$

for all $F \in \mathbb{R}^{d \times d}$ and all $R_1, R_2 \in \mathcal{SO}(d)$, and we say that W is $\mathcal{SO}(d) \times \mathcal{SO}(d)$ invariant in this case.

The following lemma shows that the lower semicontinuous polyconvex envelope of an isotropic function is again isotropic; i.e., the $\mathcal{SO}(d) \times \mathcal{SO}(d)$ invariance is preserved under polyconvexification. The similar case of $\mathcal{O}(d) \times \mathcal{O}(d)$ invariance was considered in [BDG94, Theorem 3.1], [Dac08].

LEMMA 2.1. *Let $W : \mathbb{R}^{d \times d} \to \mathbb{R}_\infty$ be isotropic. Then $W^{\mathrm{lsc\text{-}pc}}$ is isotropic.*

Proof. Let $V : \mathbb{R}^{d \times d} \to \mathbb{R}_\infty$ be lower semicontinuous polyconvex, not necessarily isotropic, with $V \leq W$, that is, $V(F) = G(\mathcal{M}(F))$ for $G : \mathbb{R}^{K_d} \to \mathbb{R}_\infty$ with G convex and lower semicontinuous on $\mathbb{R}^{K_d}$. There exists an isotropic lower semicontinuous polyconvex function V_{iso} with $V \leq V_{\mathrm{iso}} \leq W$, namely, $V_{\mathrm{iso}}(F) := \sup_{R_1, R_2 \in \mathcal{SO}(d)} V_{R_1, R_2}(F)$, where $V_{R_1, R_2}(F) = V(R_1 F R_2)$. By its definition, V_{iso} is isotropic. The lower semicontinuous polyconvexity of V_{iso} can be observed by considering $V_{R_1, R_2}(F) = G_{R_1, R_2}(\mathcal{M}(F))$ for

$$V_{R_1, R_2}(F) = \begin{cases} G_{R_1, R_2}(F, \det(F)) & \text{if } d = 2, \\ G_{R_1, R_2}(F, \mathrm{adj}(F), \det(F)) & \text{if } d = 3, \end{cases}$$

where $G_{R_1, R_2}(F, \delta) = G(R_1 F R_2, \delta)$ for $d = 2$ and $G_{R_1, R_2}(F, A, \delta) = G(R_1 F R_2, R_2^T A R_1^T, \delta)$ for $d = 3$, respectively. Here, the identities $\mathrm{adj}(R_1 F R_2) = R_2^T \mathrm{adj}(F) R_1^T$ and $\det(R_1 F R_2) = \det(F)$ for $F \in \mathbb{R}^{d \times d}$ and $R_1, R_2 \in \mathcal{SO}(d)$ have been used. It follows that G_{R_1, R_2} is convex and lower semicontinuous, and hence V_{iso} is lower semicontinuous polyconvex. Using $V \leq W$ and the isotropy of W, we observe

$$V_{\mathrm{iso}}(F) = \sup_{R_1, R_2 \in \mathcal{SO}(d)} V_{R_1, R_2}(F) \leq \sup_{R_1, R_2 \in \mathcal{SO}(d)} W(R_1 F R_2) = W(F)$$

for all $F \in \mathbb{R}^{d \times d}$, i.e., $V_{\mathrm{iso}} \leq W$. By its definition, V_{iso} is isotropic and lower semicontinuous polyconvex since convexity and lower semicontinuity are preserved for the supremum.

Consequently, it suffices to consider the supremum in (2.3) over isotropic lower semicontinuous polyconvex functions V_{iso}, i.e.,

$$W^{\text{lsc-pc}}(F) = \sup\{V(F) \mid V \text{ lsc-pc}, V \leq W\}$$
$$= \sup\{V_{\text{iso}}(F) \mid V_{\text{iso}} \text{ lsc-pc and isotropic}, V_{\text{iso}} \leq W\}.$$

This shows that $W^{\text{lsc-pc}}$ is isotropic. □

Isotropic functions can be characterized by the signed singular values of their arguments. Given $F \in \mathbb{R}^{d \times d}$ with singular values $0 \leq \sigma_1(F), \ldots, \sigma_d(F) \in \mathbb{R}^d$, the *signed singular values* $\nu_1(F) = \varepsilon_1 \sigma_1(F), \ldots, \nu_d(F) = \varepsilon_d \sigma_d(F) \in \mathbb{R}$ of F have the same absolute values as the singular values of F, and the signs $\varepsilon_1, \ldots, \varepsilon_d \in \{1, 0, -1\}$ satisfy

$$\text{sign}(\nu_1 \cdot \ldots \cdot \nu_d) = \varepsilon_1 \cdot \ldots \cdot \varepsilon_d = \text{sign}(\det(F)).$$

Note that the signed singular values are only unique up to permutations in

$$\Pi_d = \left\{ P \, \text{diag}(\varepsilon) \in \mathcal{O}(d) \mid P \in \text{Perm}(d), \varepsilon \in \{-1, 1\}^d, \varepsilon_1 \cdot \ldots \cdot \varepsilon_d = 1 \right\},$$

where $\text{diag}(\bullet)$ refers to the diagonal matrix with diagonal entries given by the vector of its argument and $\text{Perm}(d) \subset \{0, 1\}^{d \times d}$ denotes the set of permutation matrices. By means of the signed singular values, we can identify the set of isotropic functions $W : \mathbb{R}^{d \times d} \to \mathbb{R}$ with the set of Π_d-invariant functions $\Phi : \mathbb{R}^d \to \mathbb{R}_\infty$, i.e., $\Phi(\hat{\nu}) = \Phi(S\hat{\nu})$ for all $\hat{\nu} \in \mathbb{R}^d$ and all $S \in \Pi_d$. The identification is given by

$$(2.6) \qquad\qquad W(F) = \Phi(\nu(F))$$

for all $F \in \mathbb{R}^{d \times d}$ and, vice versa,

$$(2.7) \qquad\qquad \Phi(\hat{\nu}) = W(\text{diag}(\hat{\nu}))$$

for all $\hat{\nu} \in \mathbb{R}^d$.

Remark 2.2. Given this identification, we say that a Π_d-invariant function $\Phi : \mathbb{R}^d \to \mathbb{R}_\infty$ is singular value polyconvex if the corresponding W defined by (2.6) is polyconvex. Accordingly, a Π_d-invariant function Φ is called lower semicontinuous singular value polyconvex (lsc-svpc) if W is lower semicontinuous polyconvex. We define the lower semicontinuous singular value polyconvex envelope $\Phi^{\text{lsc-svpc}} : \mathbb{R}^d \to \mathbb{R}_\infty$ of Φ by

$$\Phi^{\text{lsc-svpc}}(\hat{\nu}) := \sup\{\Psi(\hat{\nu}) \mid \Psi \text{ lsc-svpc}, \Psi \leq \Phi\}.$$

This definition is justified by the natural identification of the polyconvex envelopes of an isotropic function $W : \mathbb{R}^{d \times d} \to \mathbb{R}_\infty$ and the unique Π_d-invariant function $\Phi : \mathbb{R}^d \to \mathbb{R}_\infty$ that satisfies (2.6) or, equivalently, (2.7). Then $W^{\text{lsc-pc}}$ can be identified with $\Phi^{\text{lsc-svpc}}$; i.e.,

$$W^{\text{lsc-pc}}(F) = \Phi^{\text{lsc-svpc}}(\nu(F)) \quad \text{and} \quad \Phi^{\text{lsc-svpc}}(\hat{\nu}) = W^{\text{lsc-pc}}(\text{diag}(\hat{\nu}))$$

hold for all $F \in \mathbb{R}^{d \times d}$ and for all $\hat{\nu} \in \mathbb{R}^d$.

In analogy to the original definition of polyconvexity based on the minors $\mathcal{M}$ in (2.1), we define a lifting of the arguments to a higher-dimensional space. For $d \in \{2, 3\}$,

we define $k_d := 2^d - 1$, that is, $k_d = 3$ if $d = 2$ and $k_d = 7$ if $d = 3$, and the mapping $m \colon \mathbb{R}^d \to \mathbb{R}^{k_d}$ by

$$m(\hat{\nu}) = \begin{cases} (\hat{\nu}_1, \hat{\nu}_2, \hat{\nu}_1 \hat{\nu}_2) & \text{if } d = 2, \\ (\hat{\nu}_1, \hat{\nu}_2, \hat{\nu}_3, \hat{\nu}_2 \hat{\nu}_3, \hat{\nu}_3 \hat{\nu}_1, \hat{\nu}_1 \hat{\nu}_2, \hat{\nu}_1 \hat{\nu}_2 \hat{\nu}_3) & \text{if } d = 3. \end{cases}$$

We will refer to $m(\hat{\nu})$ as the vector of minors of $\hat{\nu} \in \mathbb{R}^d$. According to [WP23], the lower semicontinuous polyconvexity of a isotropic function W can be characterized by the existence of a convex function acting on the ambient space $\mathbb{R}^{k_d}$ of the image $\mathfrak{m}_d = \{ m(\hat{\nu}) \mid \hat{\nu} \in \mathbb{R}^d \}$ of the lifting m.

THEOREM 2.3 ([WP23, Theorem 1]). *Let $d \in \{2,3\}$. An isotropic function W is lower semicontinuous polyconvex if and only if there exists a convex and lower semicontinuous function $g : \mathbb{R}^{k_d} \to \mathbb{R}_\infty$ satisfying the invariance $g(m(\hat{\nu})) = g(m(S\hat{\nu}))$ for all $S \in \Pi_d$ and all $\hat{\nu} \in \mathbb{R}^d$ such that for all F, it holds that*

(2.8) $$W(F) = g(m(\nu(F))).$$

In other words, the function W is lower semicontinuous singular value polyconvex if and only if Φ defined by (2.7) is of the form $\Phi = g \circ m$ with g convex and lower semicontinuous.

PROPOSITION 2.4. *Let $d \in \{2,3\}$. Let $W : \mathbb{R}^{d \times d} \to \mathbb{R}_\infty$ be isotropic. Define the mapping $h : \mathbb{R}^{k_d} \to \mathbb{R}_\infty$ by*

$$x \mapsto \begin{cases} W(\operatorname{diag}(\hat{\nu})) & \text{if } x = m(\hat{\nu}), \\ \infty & \text{else}, \end{cases}$$

and denote by $h^{\text{lsc-c}}$ its lower semicontinuous convex envelope. Then

$$W^{\text{lsc-pc}}(F) = h^{\text{lsc-c}}(m(\nu(F))).$$

Note that m is injective, and thus the function h is well-posed. Before we state the proof of Proposition 2.4, we want to stress the relevance of the result in the context of the Π_d-invariant function Φ, linked to W by (2.6) and (2.7).

COROLLARY 2.5. *Let $\Phi : \mathbb{R}^d \to \mathbb{R}_\infty$ be Π_d-invariant. The mapping $h : \mathbb{R}^{k_d} \to \mathbb{R}_\infty$ of Proposition 2.4 can equivalently be described by*

(2.9) $$x \mapsto \begin{cases} \Phi(\hat{\nu}) & \text{if } x = m(\hat{\nu}), \\ \infty & \text{else}. \end{cases}$$

Then the ployconvex envelope of Φ can be described by

$$\Phi^{\text{lsc-svpc}} = h^{\text{lsc-c}} \circ m.$$

Indeed, this formulation is advantageous in the numerical treatment of the problem since it is formulated for the space of signed singular values in $\mathbb{R}^d$, the domain of Φ, instead of $\mathbb{R}^{d \times d}$, the domain of W, and hence reduces dimensionality in the representative grid.

Proof of Proposition 2.4. By means of Theorem 2.3, we obtain

$$W^{\text{lsc-pc}}(F) = \sup\{ V(F) \mid V \text{ lsc-pc}, V \leq W \}$$
$$= \sup \left\{ g_{\text{sym}}(m(\nu(F))) \; \middle| \; \begin{array}{l} g_{\text{sym}} \text{ lsc-c}, g_{\text{sym}} \leq h, \\ \forall S \in \Pi_d : g_{\text{sym}} \circ m = g_{\text{sym}} \circ m \circ S \end{array} \right\}.$$

Actually, the symmetry assumption on the right-hand side is redundant due to the symmetry of h. For any lower semicontinuous and convex function $g \leq h$, define the function $g_{\mathrm{sym}} : \mathbb{R}^{k_d} \to \mathbb{R}_\infty$ with $g_{\mathrm{sym}} \circ m = g_{\mathrm{sym}} \circ m \circ S$ for all $S \in \Pi_d$ by

$$g_{\mathrm{sym}}(x) := \max_{S \in \Pi_d} \begin{cases} g(S(x_1, x_2)^\top, x_3) & \text{if } d = 2, \\ g(S(x_1, x_2, x_3)^\top, S(x_4, x_5, x_6)^\top, x_7) & \text{if } d = 3. \end{cases}$$

By construction, g_{sym} is lower semicontinuous and convex. Moreover, the Π_d-invariance of $h \circ m$ shows that for any $\hat{\nu} \in \mathbb{R}^d$,

$$g_{\mathrm{sym}}(m(\hat{\nu})) = g(m(S_{\hat{\nu}} \hat{\nu})) \leq h(m(S_{\hat{\nu}} \hat{\nu})) = h(m(\hat{\nu}))$$

holds with $S_{\hat{\nu}} = \mathrm{argmax}_{S \in \Pi_d} g(S\hat{\nu})$. It follows that $g \leq g_{\mathrm{sym}} \leq h$ and, all together, the claimed assertion holds that

$$W^{\mathrm{lsc\text{-}pc}}(F) = \sup\{g(m(\nu(F))) \mid g \text{ lsc-c}, \ g \leq h\} = h^{\mathrm{lsc\text{-}c}}(m(\nu(F))). \qquad \square$$

3. Computational signed singular value polyconvexification. The polyconvexification of a general function W acting on $d \times d$-matrices via the definition (2.5) requires, in the absence of structural properties such as isotropy, the computation of the convex envelope of a scalar function H acting essentially on a d^2-dimensional manifold in five- and 19-dimensional space for $d = 2$ and $d = 3$, respectively. So the suitable representation of W on any computational mesh already suffers severely from the high dimension, the actual computational convexification even more, no matter which algorithm is used.

This often prohibitively high computational cost can be reduced considerably under the structural assumption of isotropy. In this case, Corollary 2.5 shows that it suffices to compute the lower semicontinuous singular value polyconvex envelope of a Π_d-invariant function Φ acting on the signed singular values. This can be done by computing the convex envelope h^{c} of the function h given in (2.9). The polyconvexification of an isotropic function of dimension d thus requires only the convexification of h acting essentially on a d-dimensional manifold in three- and seven-dimensional space for $d = 2$ and $d = 3$, respectively. This drastic reduction in dimensionality makes the polyconvexification problem feasible even for $d = 3$ in many cases.

3.1. Sketch of the algorithm. Let $W : \mathbb{R}^{d \times d} \to \mathbb{R}_\infty$ be isotropic, let $\Phi : \mathbb{R}^d \to \mathbb{R}_\infty$ be the corresponding Π_d-invariant function satisfying conditions (2.6)–(2.7), and let $\hat{F} \in \mathbb{R}^{d \times d}$ have signed singular values $\hat{\nu} = \nu(\hat{F}) \in \mathbb{R}^d$. This section presents an abstract algorithm for approximating the lower semicontinuous polyconvex envelope $\Phi^{\mathrm{lsc\text{-}pc}}$ evaluated at the point $\hat{\nu}$, thus providing an approximation of the lower semicontinuous polyconvex envelope $W^{\mathrm{lsc\text{-}pc}}$ in $\hat{F}$ via $W^{\mathrm{lsc\text{-}pc}}(\hat{F}) = \Phi^{\mathrm{lsc\text{-}svpc}}(\hat{\nu})$. Since our algorithmic realization already ensures the lower semicontinuity, we abuse the notation by identifying Φ^{pc} with $\Phi^{\mathrm{lsc\text{-}svpc}}$ and W^{pc} with $W^{\mathrm{lsc\text{-}pc}}$ in the following.

As with any practical algorithm for computing (semi)convex envelopes, we assume that the set of non-polyconvexity of Φ, i.e., the support of $\Phi - \Phi^{\mathrm{pc}}$, is bounded. Without loss of generality, we assume that

$$\mathrm{supp}(\Phi - \Phi^{\mathrm{pc}}) \subset [-r, r]^d =: B(r)$$

for some bounding box $B(r)$ with radius $r > 0$. The bounding box is discretized by some grid. Although more general choices are possible, we restrict ourselves to equidistant lattices of the form

Algorithm 3.1 Signed singular value polyconvexification.

Input: $\Phi, \hat{\nu}, \delta, r$
1: $\Sigma_\delta := \delta \mathbb{Z}^d \cap B(r)$ (generate lattice in bounding box)
2: $X_\delta := m(\Sigma_\delta)$, $h_\delta := \Phi(\Sigma_\delta)$ (evaluate minors and function)
3: $h_\delta^c = \texttt{convexify}([X_\delta, h_\delta])$ (approximate convex envelope of h)
4: $\Phi_\delta^{pc}(\hat{\nu}) = \texttt{interpolate}(h_\delta^c, m(\hat{\nu}))$ (evaluate approx. polyconvex envelope at $\hat{\nu}$)
Output: $\Phi_\delta^{pc}(\hat{\nu})$

$$\Sigma_\delta = \delta \mathbb{Z}^d \cap B(r)$$

with lattice size $\delta > 0$. By $N_\delta := (2\lfloor r\delta^{-1}\rfloor + 1)^d$, we denote the total number of lattice points.

Given the function Φ; the point $\hat{\nu}$, at which the polyconvex envelope is to be approximated; and the discretization parameters δ and r, the *signed singular value polyconvexification* outlined in Algorithm 3.1 consists of four main steps.

Step 1 of Algorithm 3.1 represents the generation of the lattice Σ_δ introduced above. In an actual implementation, Σ_δ can be represented by an $N_\delta \times d$ matrix, where the rows contain the coordinates of the lattice points and induce a natural enumeration of the lattice points.

Step 2 of Algorithm 3.1 lifts the N_δ lattice points Σ_δ to the points $X_\delta := m(\Sigma_\delta)$ on the manifold $\mathfrak{m}_d$. For $d = 2$ and specific choices of r and δ, the resulting points are visualized in Figure 3.1. The lifted points form an $N_\delta \times k_d$ matrix in the implementation. In addition, the function Φ needs to be evaluated in the lattice points Σ_δ, yielding $h_\delta = \Phi(\Sigma_\delta)$, an N_δ-dimensional row vector in an implementation. At this point, possible infinite values of Φ could (and should in practice) be eliminated from h_δ as well as the corresponding points/rows from X_δ. They do not contribute to the convex envelope.

Step 3 of Algorithm 3.1 is the computation of the convex envelope of the points $(h \circ m)(\Sigma_\delta)$ representing the graph of $h \circ m$. Computationally, this can be done in several ways. The most well-known algorithm is probably the `Quickhull` algorithm [BDH96] originating from the field of computational geometry. This algorithm will be outlined in more detail in subsection 3.2 below. Alternatives for computing convex envelopes arising from other fields of mathematics include the computation of the convex envelope by its reformulation as an obstacle problem as done in [Obe07]. Suitable schemes for the resulting nonlinear partial differential equations can be used to approximate the convex envelope. Similarly, the convex envelope of a function h can be computed via a double Legendre–Fenchel conjugation due to the relation

$$h^{\text{lsc-c}} = h^{**}.$$

Algorithmic realizations of the dual Legendre–Fenchel conjugation of a discrete function h_δ have been presented, for example, in [Luc96, Luc97, CEV15]. Such approaches can benefit from parallelization, but the choice of the dual lattice is often tricky. Instead of approximating the full envelope in the bounding box, there are direct characterizations of its evaluation at $\hat{\nu}$ in terms of a linear program, as originally proposed by Bartels in the context of polyconvexity of general energy densities in [Bar05]. This variant will be discussed in more detail in subsection 3.3.

In Step 4, depending on the choice of the method `convexify` and its specific output representation, the approximate convex envelope of h at the target value $\hat{\nu}$ must
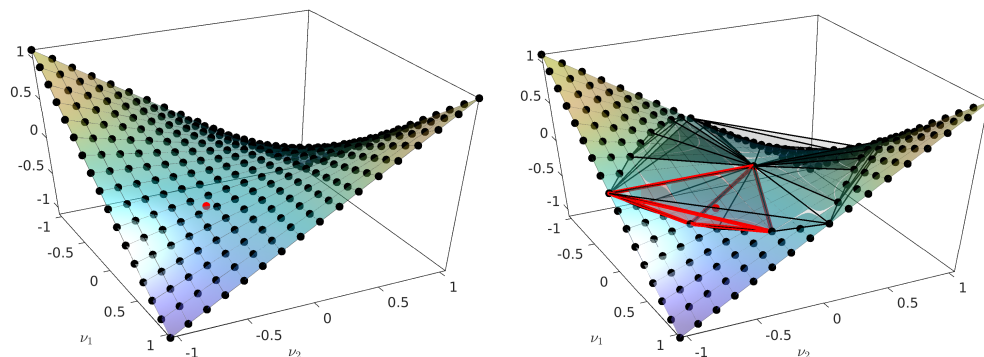
FIG. 3.1. *Discretization of signed singular values: manifold of minors $\mathfrak{m}$ (colored surface, both), lifted lattice points $X_\delta = \mathfrak{m}(\Sigma_\delta)$ (●, left), supporting points of the polyconvex envelope X_δ^c (●, right), and simplicial mesh $(\mathcal{T}_\delta, X_\delta^c)$ restricted area of non-polyconvexity (right) for the example of subsection 4.1. A sample point $\hat{\nu}$ is highlighted in both figures in red. The right figure also highlights the tetrahedron of the mesh that contains $\hat{\nu}$ and thus forms the basis for the interpolatory evaluation of the approximate polyconvex envelope in $\hat{\nu}$.*

be evaluated to obtain the desired approximation of $\Phi^{\mathrm{pc}}(\hat{\nu})$. The values h_δ^c typically represent a continuous piecewise affine function on the convex envelope, which can be represented by a simplicial mesh as illustrated in Figure 3.1. The desired approximation of $\Phi^{\mathrm{pc}}(\hat{\nu})$ can be realized by evaluating this piecewise affine function, which is achieved by the function `interpolate` in the algorithm. The practical implementation is discussed below along with the two convexification methods.

The quality of the approximation of the polyconvex envelope by Algorithm 3.1 depends on the lattice size δ. It is almost independent of the choice of `convexify`, whose error tolerances can typically be controlled reliably and accurately. The dependence of the error arising from the lattice discretization has already been quantified in [Bar05]. In our parameter setting, the original error estimate

$$(3.1) \qquad 0 \le W_{\delta,r}^{\mathrm{pc}}(F) - W^{\mathrm{pc}}(F) \le 2\,c_{\mathcal{I}}\,\delta^{1+\alpha}\,|W|_{C^{1,\alpha}(B_{r'}(0))}$$

of [Bar15, Theorem 9.10] with some interpolation constant $c_{\mathcal{I}} > 0$ can be rewritten in the isotropic setting as

$$(3.2) \qquad 0 \le \Phi_{\delta,r}^{\mathrm{pc}}(\hat{\nu}) - \Phi^{\mathrm{pc}}(\hat{\nu}) \le 2\,c_{\mathcal{I}}\,\delta^{1+\alpha}\,|\Phi|_{C^{1,\alpha}(B_{r'}(0))}.$$

3.2. Convexification by `Quickhull`. The method `convexify` in step 3 of Algorithm 3.1 computes the convex envelope of the rows of the $N_\delta \times (k_d + 1)$-matrix $p = [X_\delta, \Phi(\Sigma_\delta)]$. This computation can be translated into the geometrical framework and identified with the computation of the convex hull of the corresponding point set in $\mathbb{R}^{k_d+1}$. This issue can be addressed by a computational geometry approach; to this end, one can use the `Quickhull` algorithm [BDH96]. For point sets in dimension higher than three as in our case, it is also the most efficient one known. The algorithm follows a divide-and-conquer approach and is of complexity $\mathcal{O}(M^{\lfloor n/2 \rfloor})$, where M denotes the number of input points and n their dimension [Sei81, Cha93]. This translates to a worst-case complexity of $\mathcal{O}(N_\delta^{\lfloor (k_d+1)/2 \rfloor})$ in the present application.

The typical output representation of `Quickhull` is a simplicial mesh $\mathcal{T}_\delta^c$ of the k_d-dimensional convex hull in a $k_d + 1$-dimensional space with vertices given by the subset of the input points. This simplicial representation may not be unique unless the

vertices are in general position. However, this possible nonuniqueness in the output does not affect the convex hull. Any simplicial representation of the lower hull is perfectly fine for our purposes. Another technical problem, which is associated with this computational geometry approach, is that it does not treat the point set as the graph of a function; i.e., it returns the full convex hull of the point cloud rather than the convex envelope, which corresponds to the function. However, the convex envelope of the function can be easily extracted from the hull by computing the outer normals of the facets (which are often provided by `Quickhull` implementations anyway). If the $(k_d + 1)$st component of the normal is strictly negative, the corresponding facet is part of the envelope of the function; otherwise, it needs to be removed from the mesh.

The simplicial mesh $\mathcal{T}_\delta^c$ usually encodes the convex hull as a surface consisting of facets (k_d-simplices) by providing for each facet its $k_d + 1$ vertices as row indices of the list of supporting vertices $[X_\delta^c, h_\delta^c]$. The restriction of this mesh representation of the lower convex hull to the k_d-dimensional space is a simplicial volume mesh $(\mathcal{T}_\delta^c, X_\delta^c)$ of the convex hull of the lifted lattice points $X_\delta^c \subset \mathfrak{m}_d$, as illustrated in Figure 3.1. Thus, the values h_δ^c represent a continuous piecewise linear function on this mesh of $\mathrm{conv}(X_\delta^c)$. In step 4 of the algorithm, the evaluation of this piecewise affine function by `interpolate` can be realized as follows. A suitable search algorithm returns a simplex $\mathrm{conv}\{x_1, \ldots, x_{k_d}\} \in \mathcal{T}_\delta^c$ that contains $m(\hat{\nu})$ (the highlighted simplex in Figure 3.1). It remains to compute the barycentric coordinates $\xi_1, \ldots, \xi_{k_d} \geq 0$ of $m(\hat{\nu})$ within this simplex, which satisfy

$$(3.3) \qquad m(\hat{\nu}) = \sum_{i=1}^{k_d} \xi_i x_i, \quad \xi_1 + \ldots + \xi_{k_d} = 1.$$

Then the desired approximation of $\Phi^{\mathrm{pc}}(\hat{\nu})$ is given by

$$\Phi_\delta^{\mathrm{pc}}(\hat{\nu}) = \sum_{i=1}^{k_d} \xi_i (h_\delta^c)_i.$$

In the case that Φ attains ∞ and some grid points are removed from the discretization, $\hat{\nu}$ is not necessarily contained in a simplex of $\mathcal{T}_\delta$. This corresponds to the fact that $\Phi_\delta^{\mathrm{pc}}(\hat{\nu}) = \infty$, and this aspect has to be taken into account in the evaluation.

It is clear that the approximate polyconvex envelope can be evaluated for multiple arguments by repeated calls of the interpolation procedure but without another call to `Quickhull`. The feasibility of the resulting practical algorithm is demonstrated in the numerical experiments of subsection 4.1.

3.3. Convexification by linear programming. The computational geometry approach above aims for the convex envelope in the full bounding box. Often, we are only interested in the evaluation of an approximated envelope in a small number of points. In this case, it is useful to use the pointwise characterization of Φ^{pc} and h^c at $\hat{\nu}$ and $\hat{x} = m(\hat{\nu})$, respectively, which is given by the optimization problem

(3.4)

$$\Phi^{\mathrm{pc}}(\hat{\nu}) = h^c(\hat{x}) = \inf \left\{ \sum_{i=1}^{k_d+1} \xi_i h(x_i) \,\middle|\, \xi_i \in [0,1], \, x_i \in \mathbb{R}^{k_d}, \, \sum_{i=1}^{k_d+1} \xi_i = 1, \, \sum_{i=1}^{k_d+1} \xi_i x_i = \hat{x} \right\}.$$

The formula for the convex envelope of h can be found in [Dac08, Theorem 2.35], while the reformulation for the polyconvex envelope for not necessarily isotropic W

was derived in [Bar05]. After suitable discretization of $\mathbb{R}^{k_d}$, e.g., by the lifted lattice $m(\Sigma_\delta) = X_\delta = \{x_i\}_{i=1}^{N_\delta}$, this nonlinear optimization problem turns into the following linear program:

$$(3.5) \qquad \Phi_\delta^{\mathrm{pc}}(\hat{\nu}) = h_\delta^{\mathrm{c}}(\hat{x}) = \min\left\{ \sum_{i=1}^{N_\delta} \xi_i\, h(x_i) \,\bigg|\, \xi_i \geq 0,\ \sum_{i=1}^{N_\delta} \xi_i = 1,\ \sum_{i=1}^{N_\delta} \xi_i x_i = \hat{x} \right\}.$$

Possible infinite values of $h(x_i) = h(m(\nu_i)) = \Phi(\nu_i)$ should be avoided by removing the corresponding vertices from the lattice as discussed earlier. Rather than first computing the full convex envelope and then searching for a facet that contains $\hat{x} = m(\hat{\nu})$ as in Figure 3.1, this approach directly computes that facet. In exact arithmetic, there exists a minimizer ξ with at most $k_d + 1$ nonzero entries that represents the barycentric coordinates of $\hat{x}$ with respect to the vertices of the k_d-simplex. Up to the possible nonuniqueness of the $k_d + 1$ indices, which corresponds to nonzero entries, and the simplicial mesh representation of the convex envelope, these vertices x_i and the corresponding nonzero coefficients ξ_i coincide with those of (3.3). The linear program (3.5) can be solved fairly efficiently by standard algorithms for linear programming available in various software libraries. In [Bar05], an active set strategy along with multilevel optimization and adaptive techniques were suggested to improve the runtime in the setting of general nonisotropic functions further. We will use the algorithm along with the MATLAB function for linear programming in the numerical experiments of section 4.

4. Numerical experiments. In this section, we illustrate the performance of the presented singular value polyconvexification algorithm with a number of numerical examples. Due to the requirement of isotropy, we restrict ourselves to functions that satisfy this condition. In our experiments, we use Algorithm 3.1 with both `Quickhull` and the linear programming approach for convexification as discussed in subsections 3.2 and 3.3, respectively. Further, we apply both approaches also for the complete matrix case by convexifying (2.4) in order to investigate the computational speedup resulting from the dimension reduction.

A basic MATLAB [Mat22] implementation of the two variants of Algorithm 3.1 and their application to the examples of subsections 4.1 and 4.2 is available as supplementary material (supplCodeCompPolyOfIsoFunct.zip [local/web 2.50KB]). We use the MATLAB internal implementation of the `Quickhull` algorithm as well as the `Interior-Point-Legacy` method for solving the linear program (3.5) using `linprog`. The MATLAB implementation with application to the benchmark examples can also be found at https://github.com/TmNmr/SVPC.

4.1. Kohn–Strang–Dolzmann example. The following example was studied in [KS86a, KS86b], subsequently modified to achieve continuity in [Dol99, DW00], and further studied in [Bar05]. We consider the function $W : \mathbb{R}^{2\times 2} \to \mathbb{R}$, defined as

$$W(F) := \begin{cases} 1 + |F|^2 & \text{if } |F| \geq \sqrt{2} - 1, \\ 2\sqrt{2}\,|F| & \text{if } |F| \leq \sqrt{2} - 1, \end{cases}$$

where $|F| := (\sum_{i,j=1}^d F_{ij}^2)^{1/2}$ denotes the Frobenius norm of F. The polyconvex hull of W is explicitly known and reads

$$W^{\mathrm{pc}}(F) = \begin{cases} 1 + |F|^2 & \text{if } \varrho \geq 1, \\ 2\,(\varrho(F) - |\det(F)|) & \text{if } \varrho \leq 1, \end{cases}$$
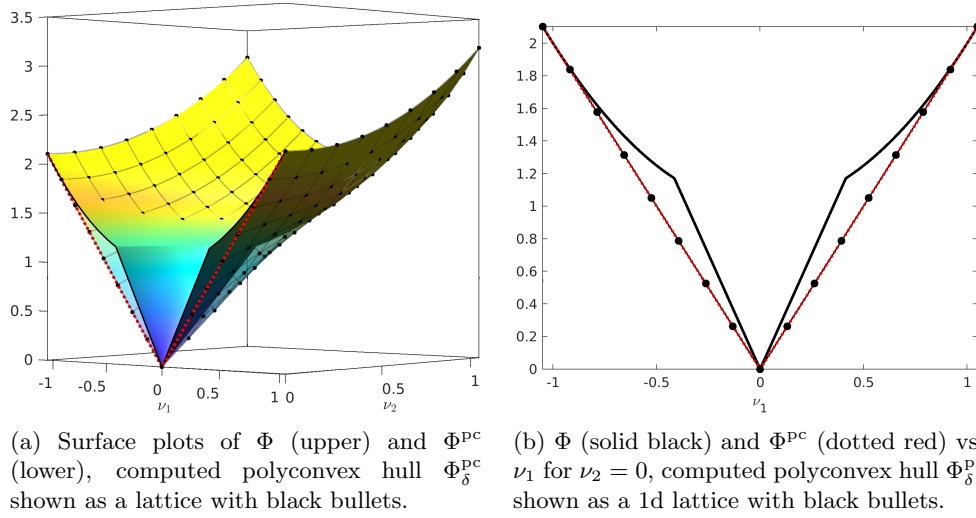
(a) Surface plots of Φ (upper) and Φ^{pc} (lower), computed polyconvex hull $\Phi_\delta^{\mathrm{pc}}$ shown as a lattice with black bullets.

(b) Φ (solid black) and Φ^{pc} (dotted red) vs. ν_1 for $\nu_2 = 0$, computed polyconvex hull $\Phi_\delta^{\mathrm{pc}}$ shown as a 1d lattice with black bullets.

FIG. 4.1. *Illustration of function Φ from* (4.1), *its polyconvex hull Φ^{pc} from* (4.2), *and computed polyconvex hull $\Phi_\delta^{\mathrm{pc}}$ using* `Quickhull` *and discretization parameters $r = 1.05$, $\delta = 0.13125$, using $N_\delta = 17^2$ lattice points.*

where $\varrho(F) := \sqrt{|F|^2 + 2\,|\det F|}$. Note that $W^{\mathrm{pc}} \neq W^{\mathrm{c}}$ in this example. The functions W and W^{pc} are isotropic, and, rewritten in terms of the signed singular values, they reduce to $\Phi, \Phi^{\mathrm{pc}} : \mathbb{R}^2 \to \mathbb{R}$ with

(4.1)
$$\Phi(\hat\nu) := \begin{cases} 1 + \nu_1^2 + \nu_2^2 & \text{if } \sqrt{\nu_1^2 + \nu_2^2} \geq \sqrt{2} - 1, \\ 2\sqrt{2}\,\sqrt{\nu_1^2 + \nu_2^2} & \text{if } \sqrt{\nu_1^2 + \nu_2^2} \leq \sqrt{2} - 1 \end{cases}$$

and

(4.2)
$$\Phi^{\mathrm{pc}}(\hat\nu) = \begin{cases} 1 + \nu_1^2 + \nu_2^2 & \text{if } \varrho \geq 1, \\ 2\,(|\nu_1| + |\nu_2| - |\nu_1\,\nu_2|) & \text{if } \varrho \leq 1 \end{cases}$$

with $\varrho(\hat\nu) = |\nu_1| + |\nu_2|$. Figure 4.1 shows the function Φ, its polyconvex envelope Φ^{pc}, and the computed approximation $\Phi_\delta^{\mathrm{pc}}$ resulting from Algorithm 3.1 with `Quickhull` as outlined in subsection 3.2. Note that Figure 4.1(a) still shows nonconvexity of $\Phi_\delta^{\mathrm{pc}}$ along the diagonal $\nu_1 = \nu_2$, which is in line with the nonconvexity of Φ^{pc}. In Figure 4.2, we compare this variant of the algorithm (referred to as svpc QH) with the variant based on linear programming (svpc LP) described in subsection 3.3. For reference, we also show the results for the corresponding algorithms for the polyconvex hull W without exploiting isotropy. As a linear programming variant of the polyconvexification of W, we use the adaptive algorithm of [Bar05] and its implementation presented in [Bar15] (denoted pc [Bar05]). We also implemented the direct convexification of W using `Quickhull`, which convexifies H in (2.5) (pc QH). All simulations were performed on a state-of-the-art laptop computer.

The left graph in Figure 4.2 shows absolute errors in evaluating the polyconvex hull at the point

$$\hat{F} = \begin{bmatrix} 0.2 & 0.1 \\ 0.1 & 0.3 \end{bmatrix}$$
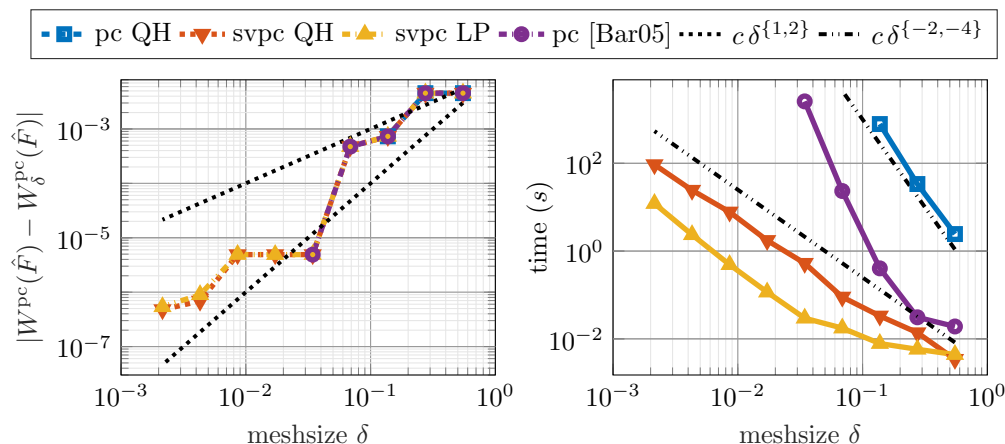
FIG. 4.2. *Quantitative comparison of computational polyconvexification of the Kohn–Strang–Dolzmann example of section* 4.1 *in the matrix* $\hat{F}$ *and known exact values* $W(\hat{F}) \approx 1.095$ *and* $W^{\mathrm{pc}}(\hat{F}) = 0.9$. *Left: absolute error with respect to lattice parameter* δ *for several methods. Right: corresponding computing times.*

with singular values $\hat{\nu}_1 \approx 0.3618$ and $\hat{\nu}_2 \approx 0.1282$. For fixed $r = 1.1$, the presented algorithms indeed converge at a rate $\delta^{1+\alpha}$ for some $\alpha \in [0, 1]$ as the lattice parameter δ is refined, in agreement with theoretical predictions (3.1)–(3.2).

Although the algorithms are virtually equally accurate, they differ significantly in computational complexity. With the exception of the pc [Bar05] variant, computation times actually scale only linearly with the number of grid points, which in turn is proportional to δ^{-4} for pc QH and δ^{-2} for svpc QH and svpc LP. This is much better than the worst-case complexity of `Quickhull`, which predicts δ^{-8} and δ^{-4} for pc QH. The observed behavior seems to correspond to the `Quickhull` complexity in the dimensional space 4 or 2, which represents the dimensions of the manifolds and not the ambient space.

In any case, the numerical results clearly demonstrate the claimed superiority of the new algorithms in the isotropic regime. Of the two variants of singular value polyconvexity, the linear programming variant appears to be faster for our implementation. Note, however, that `Quickhull` approximates the envelope throughout the bounding box, and it would easily pay off if the polyconvex envelope were evaluated at multiple points.

4.2. Multidimensional double-well potential. Since the generalization of the previous example to three dimensions is not known explicitly, we consider the function

$$W : \mathbb{R}^{d \times d} \to \mathbb{R}$$
$$F \mapsto \left(|F|^2 - 1 \right)^2,$$

which is an established benchmark for analytical and computational semiconvexification [KS86a, DW00, Bar05]. For any $d \in \{1, 2, 3\}$, the rank-one, the quasiconvex, and the polyconvex envelope of W coincide with the convex envelope given by

$$W^{\mathrm{pc}}(F) = \begin{cases} \left(|F|^2 - 1 \right)^2 & \text{if } |F| \geq 1, \\ 0 & \text{else.} \end{cases}$$
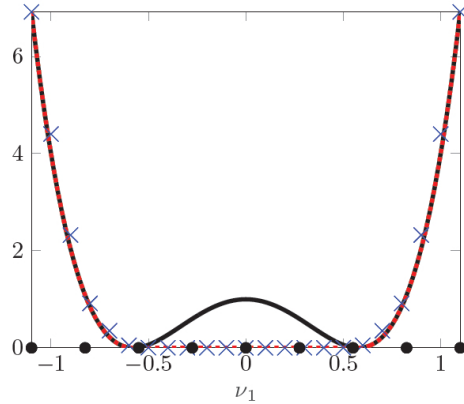
FIG. 4.3. *Slice of the three-dimensional double-well example. Function Φ (4.3) (solid black), its polyconvex hull Φ^{pc} (4.4) (dotted red) versus $\nu_1 = \nu_2 = \nu_3$, evaluation of polyconvex hull $\Phi_\delta^{\mathrm{pc}}$ via svpc LP (3.5) (blue crosses), and a selection of lattice points involved in the minimization problem (black bullets).*

The function W is isotropic and can be reformulated in terms of the signed singular values via the function Φ by

$$(4.3) \qquad \Phi(\hat{\nu}) = \left(\sum_{i=1}^d \nu_i^2 - 1 \right)^2.$$

Similarly, the polyconvex hull of Φ can be expressed as

$$(4.4) \qquad \Phi^{\mathrm{pc}}(\hat{\nu}) = \begin{cases} \left(\sum_{i=1}^d \nu_i^2 - 1 \right)^2 & \text{if } \sum_{i=1}^d \nu_i^2 \geq 1, \\ 0 & \text{else.} \end{cases}$$

An illustration of the function Φ and the computed envelope $\Phi_\delta^{\mathrm{pc}}$ for three spatial dimensions is given in Figure 4.3. The slice along the diagonal direction $\nu_1 [1, 1, 1]^T$ is plotted. The calculation via the svpc LP approach is based on the lattice characterized by $\delta = 0.28125$ and the radius $r = 1.125$. In total, $9^3 = 729$ lattice points are involved in the minimization problem. A selection of those lattice points is marked by black bullets, exactly the ones lying on the diagonal slice. The sequential pointwise evaluation of $\Phi_\delta^{\mathrm{pc}}$ is marked by blue crosses.

Given the performance of the algorithms in the two-dimensional example of subsection 4.1, we restrict the quantitative study of convergence and complexity to the linear programming variant of Algorithm 3.1. For $d = 2$ and $d = 3$, absolute errors and computing times are shown in Figure 4.4 relative to the lattice parameter δ. The radius of the bounding box is set to $r = 2$. For this particularly smooth energy density and polyconvex envelope, the convergence of the error in the points

$$\hat{F} = \begin{bmatrix} 0.2 & 0.1 \\ 0.1 & 0.3 \end{bmatrix}$$

and $\hat{F} = \mathrm{diag}(0.3, 0.3, 0.3)$ is faster than expected, proportional to δ^4 in both the two- and the three-dimensional case. The corresponding computing times scale linearly and thus optimal in the number of lattice points; i.e., they are proportional to δ^{-d} for $d = 2, 3$. However, in general, this behavior is limited to this benchmark example, which is more of theoretical interest.
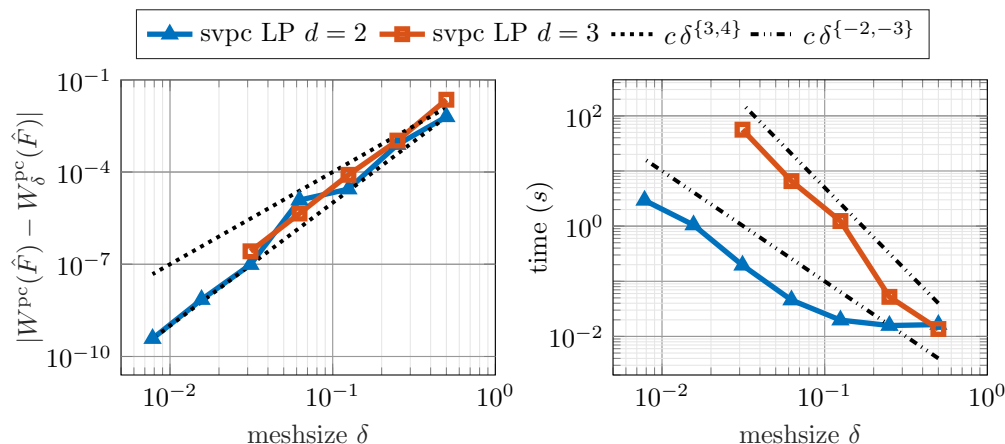
Fig. 4.4. *Quantitative comparison of computational polyconvexification via the svpc LP approach of the two- and three-dimensional double-well example of section 4.2 in the matrix $\hat{F}$. Left: absolute error with respect to lattice parameter δ for $d \in \{2,3\}$. Right: corresponding computing times.*

4.3. Saint Venant–Kirchhoff. The next example shows the application to functions of more relevance in real-world applications. We consider the well-known Saint Venant–Kirchhoff energy density. It is given by

$$W(F) = \frac{E}{8(1+\tilde{\nu})}\|F^T F - I\|^2 + \frac{E\tilde{\nu}}{8(1+\tilde{\nu})(1-2\tilde{\nu})}\left(\|F\|^2 - 3\right)^2,$$

where $E > 0$ is Young's modulus and $0 \leq \tilde{\nu} < 1/2$ is Poisson's ratio. Rewriting this function in terms of the singular values leads to

$$W(F) = \frac{E}{8(1+\tilde{\nu})}\sum_{i=1}^{3}(\sigma_i(F)^2 - 1)^2 + \frac{E\tilde{\nu}}{8(1+\tilde{\nu})(1-2\tilde{\nu})}\left(\sum_{i=1}^{3}\left(\sigma_i(F)^2 - 1\right)\right)^2.$$

From [LDR95], it is known that the polyconvex envelope is of the form

$$W^{\mathrm{pc}}(F) = \Psi(\sigma_1(F), \sigma_2(F), \sigma_3(F)),$$

where $0 \leq \sigma_1(F) \leq \sigma_2(F) \leq \sigma_3(F)$ denote the singular values of F and $\Psi : \mathbb{R}^3 \to \mathbb{R}$ is defined by

$$\Psi(\hat{\sigma}) = \frac{E}{8}[\sigma_3^2 - 1]_+^2 + \frac{E}{8(1-\tilde{\nu}^2)}[\sigma_2^2 + \tilde{\nu}\sigma_3^2 - (1+\tilde{\nu})]_+^2$$
$$+ \frac{E}{8(1-\tilde{\nu}^2)(1-2\tilde{\nu})}[(1-\tilde{\nu})\sigma_1^2 + \tilde{\nu}(\sigma_2^2 + \sigma_3^2) - (1+\tilde{\nu})]_+^2.$$

Here, $[a]_+^2$ is a^2 if $a \geq 0$ and 0 if $a < 0$.

This function separates the tetrahedral cone $0 \leq \nu_1 \leq \nu_2 \leq \nu_3$ into four parts. The evaluation point $\hat{F} = \mathrm{diag}(0.2, 0.4, 1.5)$ is located in a part where Ψ and hence W^{pc} are not constant zero. Figure 4.5 shows the approximation error and corresponding computation times utilizing the linear programming approach in Algorithm 3.1. We choose material parameters $E = 1$, $\nu = 1/4$ and discretization radius $r = 2$. Quadratic error convergence in the mesh size can be observed as well as a scaling of computation times of the order of between δ^{-5} and δ^{-6}. This reflects the challenges that arise
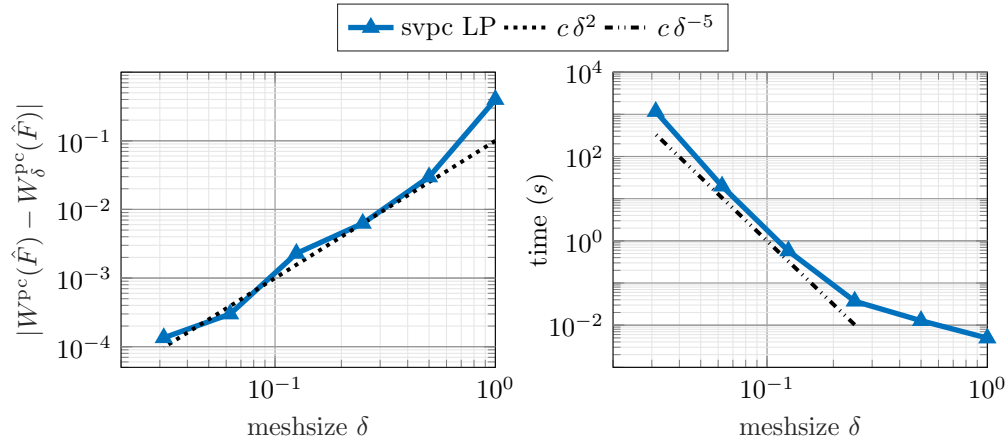
FIG. 4.5. *Quantitative study of computational polyconvexification via the svpc LP approach of the three-dimensional Saint Venant–Kirchhoff example of section 4.3 in the matrix $\hat{F}$. Left: absolute error with respect to lattice parameter δ. Right: corresponding computing times.*

when dealing with more realistic energy densities and indicates that the application of standard $d \times d$ algorithms would not be possible due to the computational complexity. However, the presented algorithm successfully performs a convexification of physically relevant isotropic functions in the three-dimensional case, which is hardly feasible without exploiting isotropy.

4.4. Exponentiated Hencky-logarithmic energies. The new efficient algorithms for polyconvexication of isotropic energies allow us to shed light on a family of exponentiated Hencky-type energies $W_{\mathrm{eH}} : \mathbb{R}^{d\times d} \to \mathbb{R}_\infty$ recently proposed by [NLG$^+$15]. Given parameters $\mu, \kappa, k, \ell > 0$, they are given by

$$W_{\mathrm{eH}}(F) = \begin{cases} \dfrac{\mu}{k} e^{k\|\operatorname{dev}_d \log U\|^2} + \dfrac{\kappa}{2\ell} e^{\ell[\log \det U]^2} & \text{if } \det(F) > 0, \\ \infty & \text{if } \det(F) \leq 0, \end{cases}$$

where $U := \sqrt{F^T F}$, $\log X$ is the matrix logarithm and $\operatorname{dev}_d X = X - \frac{1}{d}\operatorname{tr}(X)I_d$ is the deviatoric part of a matrix $X \in \mathbb{R}^{d\times d}$. In the two-dimensional case, [NLG$^+$15, Theorem 3.11] shows that if $k \geq \frac{1}{3}$ and $\ell \geq \frac{1}{8}$, then W_{eH} is polyconvex. We will study the sharpness of this result using our algorithm. For this purpose, W_{eH} is rephrased for the case $d = 2$ in terms of signed singular values as

$$(4.5) \qquad \Phi_{\mathrm{eH}}(\hat{\nu}) = \begin{cases} \dfrac{\mu}{k} e^{\frac{k}{2}(\log \frac{\nu_1}{\nu_2})^2} + \dfrac{\kappa}{2\ell} e^{\ell(\log(\nu_1 \nu_2))^2} & \text{if } \nu_1 \nu_2 > 0, \\ \infty & \text{else.} \end{cases}$$

Figure 4.6 shows contour plots of the difference $|\Phi_{\mathrm{eH}} - \Phi_{\mathrm{eH},\delta}^{\mathrm{pc}}|$ on the quadrant of positive signed singular values for parameters $\mu = 1$ and $\kappa = 1$ and three configurations for the parameter pair (ℓ, k). The approximation $\Phi_{\mathrm{eH},\delta}^{\mathrm{pc}}$ was computed by the `Quickhull` approach on a grid with radius $r = 12$. Note that the nonconvex regime of Φ_{eH} is indeed larger than the area covered by the ball of radius $r = 12$. However, we are only interested in the loss of polyconvexity in the neighborhood of the identity (the point $\nu_1 = \nu_2 = 1$) since the application in boundary value problems would also be in a ball of finite radius.

From Figure 4.6, it is clearly visible that each of the two parameters k and ℓ triggers a certain region of non-polyconvexity in the space of signed singular values. To investigate this further, we fix the material parameters $\mu = 1$ and $\kappa = 1$ and study the
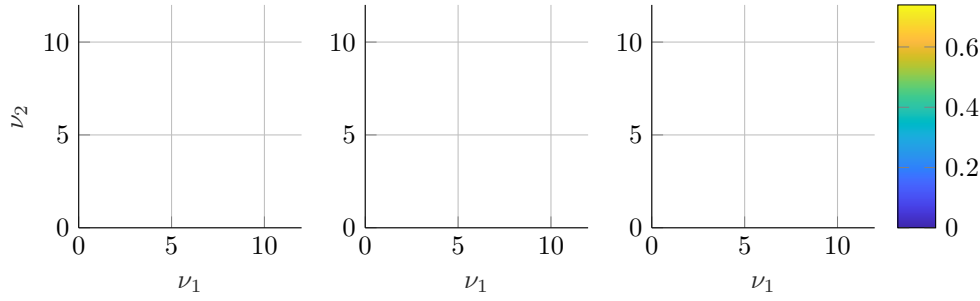
FIG. 4.6. $|\Phi_{eH} - \Phi_{eH,\delta}^{\mathrm{pc}}|$ on $\mathcal{N}_{\delta,r}$ for parameter pairs $(\ell, k) = (0.06, 1/3)$ on the left, $(0.06, 0.06)$ in the middle, and $(1/8, 0.06)$ on the right. Discretization parameters for the svpc QH approach were $r = 12$ and $\delta = 0.09375$.
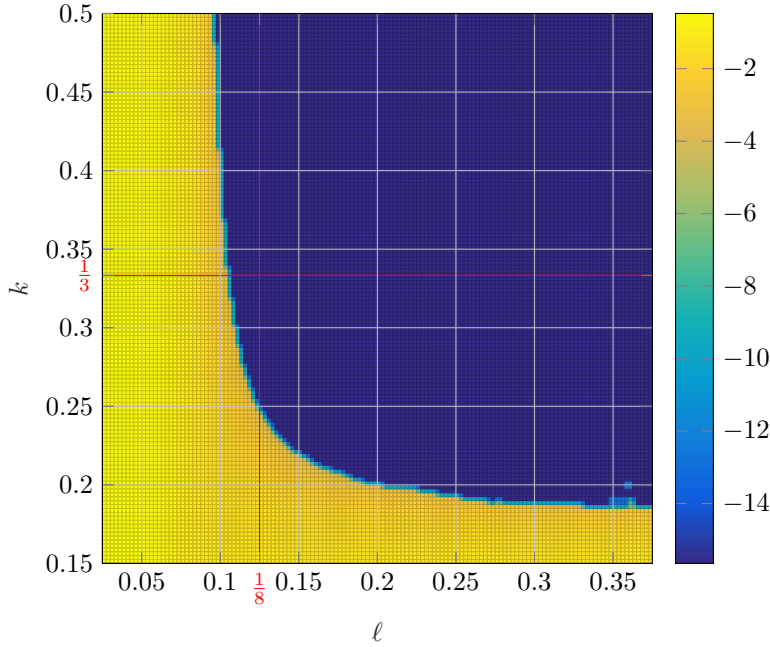

FIG. 4.7. Comparison of Φ_{eH} and $\Phi_{eH,\delta}^{\mathrm{pc}}$ for varying parameters k, ℓ and $\mu = 1, \kappa = 1$. Plot shows $\log_{10} |\Phi_{eH} - \Phi_{eH,\delta}^{\mathrm{pc}}|_\infty$. Red lines indicate analytically known parameter bounds. k, ℓ axes are discretized with stepsize of 0.0025. Each polyconvexification has been carried out with discretization parameters $r = 8.0$, $\delta = 0.1250$, corresponding to refinement level 7.

polyconvexity of Φ_{eH} depending on the parameters k and ℓ. We choose a bounding box of radius $r = 8$ and fix the lattice parameter to $\delta = 0.1250$. We compute the polyconvex envelope in all lattice points using the `Quickhull` approach and compute the maximal absolute error between this approximate polyconvex hull and the original function. Errors at the order of the lattice parameter indicate polyconvexity of the original function, while significantly larger errors indicate non-polyconvexity. These results confirm the polyconvexity of W_{eH} if $k \geq \frac{1}{3}$ and $\ell \geq \frac{1}{8}$ as shown in [NLG+15]. Moreover, our numerical investigations show that the restriction of W_{eH} to the bounded box $\nu_1, \nu_2 \leq r$ is also polyconvex for values $k < \frac{1}{3}$ and $\ell < \frac{1}{8}$. For fixed μ and κ, the bounds might be relaxed as visualized in Figure 4.7.

5. Conclusion. We have shown that the computational efficiency of algorithms for polyconvex isotropic energy densities can be significantly improved. Based on the characterization of isotropic polyconvexity in terms of the signed singular values instead of the full matrix input [WP23], we have shown how the corresponding dimensional reduction from d^2- to d-dimensional space can be realized algorithmically. The convexification of the lifted space can be performed by computational geometry algorithms or linear programming. Both variants not only have minimal complexity in representative benchmarks but also allow numerical investigation of exponentiated Hencky-logarithmic energy densities and their polyconvexity properties for a range of parameters beyond those known analytically.

REFERENCES

[AF84]   E. ACERBI AND N. FUSCO, *Semicontinuity problems in the calculus of variations*, Arch. Ration. Mech. Anal., 86 (1984), pp. 125–145.

[Bal76] J. M. BALL, *Convexity conditions and existence theorems in nonlinear elasticity*, Arch. Ration. Mech. Anal., 63 (1976), pp. 337–403.

[Bal77] J. M. BALL, *Constitutive inequalities and existence theorems in nonlinear elastostatics*, in Nonlinear Analysis and Mechanics: Heriot-Watt Symposium, Vol. 1, Pitman Research Notes in Mathematics Series 17, R. J. Knops, ed., Pitman Books, London, 1977, pp. 187–241.

[Bal02] J. M. BALL, *Some Open Problems in Elasticity*, Springer-Verlag, Berlin, 2002, pp. 3–59.

[Bar05] S. BARTELS, *Reliable and efficient approximation of polyconvex envelopes*, SIAM J. Numer. Anal., 43 (2005), pp. 363–385.

[Bar15] S. BARTELS, *Numerical Methods for Nonlinear Partial Differential Equations*, Springer Series in Computational Mathematics 47, Springer-Verlag, Berlin, 2015.

[BCHH04] S. BARTELS, C. CARSTENSEN, K. HACKL, AND U. HOPPE, *Effective relaxation for microstructure simulations: Algorithms and applications*, Comput. Methods Appl. Mech. Engrg., 193 (2004), pp. 5143–5175.

[BDG94] G. BUTTAZZO, B. DACOROGNA, AND W. GANGBO, *On the envelopes of functions depending on singular values of matrices*, Boll. Unione Mat. Ital. VII. Ser. B, 8 (1994), pp. 17–35.

[BDH96] C. B. BARBER, D. P. DOBKIN, AND H. HUHDANPAA, *The quickhull algorithm for convex hulls*, ACM Trans. Math. Software, 22 (1996), pp. 469–483.

[BEG15] T. BOSSE, L. ENEYA, AND A. GRIEWANK, *An algorithm for pointwise evaluation of polyconvex envelopes* II*: Generalization and numerical results*, Afr. Mat., 26 (2015), pp. 31–52.

[BKN+23] D. BALZANI, M. KÖHLER, T. NEUMEIER, M. A. PETER, AND D. PETERSEIM, *Multidimensional rank-one convexification of incremental damage models at finite strains*, Comput. Mech., 73 (2023), pp. 27–47.

[BKS19] O. BOUSSAID, C. KREISBECK, AND A. SCHLÖMERKEMPER, *Characterizations of symmetric polyconvexity*, Arch. Ration. Mech. Anal., 234 (2019), pp. 417–451.

[BO12]   D. BALZANI AND M. ORTIZ, *Relaxed incremental variational formulation for damage at large strains with application to fiber-reinforced materials and materials with truss-like microstructures*, Internat. J. Numer. Methods Engrg., 92 (2012), pp. 551–570.

[CD18]   S. CONTI AND G. DOLZMANN, *An adaptive relaxation algorithm for multiscale problems and application to nematic elastomers*, J. Mech. Phys. Solids, 113 (2018), pp. 126–143.

[CEV15] L. CONTENTO, A. ERN, AND R. VERMIGLIO, *A linear-time approximate convex envelope algorithm using the double Legendre–Fenchel transform with application to phase separation*, Comput. Optim. Appl., 60 (2015), pp. 231–261.

[Cha93] B. CHAZELLE, *An optimal convex hull algorithm in any fixed dimension*, Discrete Comput. Geom., 10 (1993), pp. 377–409.

[Dac82] B. DACOROGNA, *Quasiconvexity and relaxation of nonconvex problems in the calculus of variations*, J. Funct. Anal., 46 (1982), pp. 102–118.

[Dac08]   B. DACOROGNA, *Direct Methods in the Calculus of Variations*, Applied Mathematical
           Sciences 78, Springer-Verlag, Berlin, 2008.
[DM06]   B. DACOROGNA AND P. MARÉCHAL, *A note on spectrally defined polyconvex functions*,
           in Proceedings of the Workshop "New Developments in the Calculus of Variations,"
           2006, pp. 259–274.
[Dol99]   G. DOLZMANN, *Numerical computation of rank-one convex envelopes*, SIAM J. Numer.
           Anal., 36 (1999), pp. 1621–1635.
[DW00]   G. DOLZMANN AND N. J. WALKINGTON, *Estimates for numerical approximations of rank
           one convex envelopes*, Numer. Math., 85 (2000), pp. 647–663.
[EBG13]   L. ENEYA, T. BOSSE, AND A. GRIEWANK, *A method for pointwise evaluation of polyconvex
           envelopes*, Afr. Mat., 24 (2013), pp. 1–24.
[KNM⁺22]   M. KÖHLER, T. NEUMEIER, J. MELCHIOR, M. A. PETER, D. PETERSEIM, AND D. BALZANI,
           *Adaptive convexification of microsphere-based incremental damage for stress and
           strain softening at finite strains*, Acta Mech., 233 (2022), pp. 4347–4364.
[KNP⁺23]   M. KÖHLER, T. NEUMEIER, D. PETERSEIM, M. A. PETER, AND D. BALZANI, *Relaxed in-
           cremental formulations for damage at finite strains including strain softening*, Proc.
           Appl. Math. Mech., 23 (2023), e202200297.
[KS86a]   R. V. KOHN AND G. STRANG, *Optimal design and relaxation of variational problems*, I,
           Comm. Pure Appl. Math., 39 (1986), pp. 113–137.
[KS86b]   R. V. KOHN AND G. STRANG, *Optimal design and relaxation of variational problems*, II,
           Comm. Pure Appl. Math., 39 (1986), pp. 139–182.
[LDR95]   H. L. DRET AND A. RAOULT, *The quasiconvex envelope of the Saint Venant–Kirchhoff
           stored energy function*, Proc. Roy. Soc. Edinburgh Sect. A, 125 (1995), pp. 1179–
           1192.
[Luc96]   Y. LUCET, *A fast computational algorithm for the Legendre-Fenchel transform*, Comput.
           Optim. Appl., 6 (1996), pp. 27–57.
[Luc97]   Y. LUCET, *Faster than the fast Legendre transform, the linear-time Legendre transform*,
           Numer. Algorithms, 16 (1997), pp. 171–185.
[Mat22]   The MathWorks, *Matlab version 9.13.0 (r2022b)*, 2022.
[Mie05]   A. MIELKE, *Necessary and sufficient conditions for polyconvexity of isotropic functions*,
           J. Convex Anal., 12 (2005), pp. 291–314.
[Mül99]   S. MÜLLER, *Variational Models for Microstructure and Phase Transitions*, Springer-
           Verlag, Berlin, 1999, pp. 85–210.
[NLG⁺15]   P. NEFF, J. LANKEIT, I.-D. GHIBA, R. MARTIN, AND D. STEIGMANN, *The exponenti-
           ated Hencky-logarithmic strain energy. Part* II*: Coercivity, planar polyconvexity and
           existence of minimizers*, Z. Angew. Math. Phys., 66 (2015), pp. 1671–1693.
[Obe07]   A. M. OBERMAN, *The convex envelope is the solution of a nonlinear obstacle problem*,
           Proc. Amer. Math. Soc., 135 (2007), pp. 1689–1694.
[Rao86]   A. RAOULT, *Non-polyconvexity of the stored energy function of a Saint Venant–Kirchhoff
           material*, Apl. Mat., 31 (1986), pp. 417–419.
[Ros98]   P. ROSAKIS, *Characterization of convex isotropic functions*, J. Elasticity, 49 (1997/98),
           pp. 257–267.
[Rou20]   T. ROUBÍČEK, *Relaxation in Optimization Theory and Variational Calculus*, De Gruyter,
           Berlin, 2020.
[Sei81]   R. SEIDEL, *A Convex Hull Algorithm Optimal for Point Sets in Even Dimensions*, Tech-
           nical report, CAN, 1981.
[Š97]   M. ŠILHAVÝ, *The Mechanics and Thermodynamics of Continuous Media*, Texts and Mono-
           graphs in Physics, Springer-Verlag, Berlin, 1997.
[Š99]   M. ŠILHAVÝ, *Convexity conditions for rotationally invariant functions in two dimensions*,
           in Applied Nonlinear Analysis, Kluwer/Plenum, Dordrecht, the Netherlands, 1999,
           pp. 513–530.
[WP23]   D. WIEDEMANN AND M. A. PETER, *Characterization of Polyconvex Isotropic Functions*,
           arXiv:2304.08385, 2023.